applied sciences

Article

Fuzzy and Neural Network Approaches to Wind Turbine Fault Diagnosis

Saverio Farsoni [1,†], Silvio Simani [1,†*] and Paolo Castaldi [2]

[1] Department of Engineering, University of Ferrara; {saverio.farsoni,silvio.simani}@unife.it
[2] Department of Electrical, Electronic, and Information Engineering, University of Bologna; paolo.castaldi@unife.it
* Correspondence: silvio.simani@unife.it; Tel.: +39-0532-97-4844 (F.L.)
† Current address: Ferrara, Via Saragat 1E. I–44122. Ferrara, FE, Italy

Abstract: The fault diagnosis of safety critical systems such as wind turbine installations includes extremely challenging aspects that motivate the research issues considered in this paper. In fact, the prompt detection and the reliable diagnosis of faults in their earlier occurrence represent the key point especially for offshore installations. For these plants, operation and maintenance procedures in harsh environments would inevitably increase the cost of the energy production. Therefore, this work investigates fault diagnosis solutions that are considered in a viable way and used as advanced techniques for condition monitoring of dynamic processes. To this end, the work proposes the design of fault diagnosis strategies that exploit the estimation of the fault by means of data–driven approaches. This solution leads to the development of effective methods allowing the management of partially unknown information of the system dynamics, while coping with measurement errors, the model–reality mismatch and other disturbance effects. In mode detail, the proposed data–driven methodologies exploit fuzzy systems and neural networks in order to estimate the nonlinear dynamic relations between the input and output measurements of the considered process and the faults. To this end, the fuzzy and neural network structures are integrated with auto–regressive with exogenous input descriptions, thus making them able to approximate unknown nonlinear dynamic functions with arbitrary degree of accuracy. Once these models are estimated from the input and output data measurement acquired from the considered dynamic process, the capabilities of their fault diagnosis capabilities are validated by using a high–fidelity benchmark that simulates the healthy and the faulty behaviour of a wind turbine system. Moreover, at this stage the benchmark is also useful to analyse the robustness and the reliability characteristics of the developed tools in the presence of model–reality mismatch and modelling error effects featured by the wind turbine simulator. On the other hand, a hardware–in–the–loop tool is finally implemented for testing and comparing the performance of the developed fault diagnosis strategies in a more realistic environment and with respect to different fault diagnosis approaches.

Keywords: fuzzy systems; neural networks; fault diagnosis; data–driven approaces; robustness and reliability; wind turbine

1. Introduction

Wind power is the second largest source of renewable energy after solar power sources globally. The global popularity of wind power has risen significantly due to the need to harness electrical power from renewable sources in order to limit and end the necessity of the fossil fuels [1]. Variable–speed wind turbines are the most important component of a Wind Energy Conversion System (WECS). For effective and reliable power conversion, suitable technical and technological solutions have to be properly implemented and exploited in WECSs.

 doi:10.20944/preprints202105.0315.v1

Technological advances in wind power generation systems have encouraged the installation of wind farms. Owing to the large size and requirement of high wind speeds, these installations are located in offshore areas. Such installations of offshore WECS result in disadvantages such as high expense to install, and the non–availability of continuous supervision, Operation and Maintenance (O&M), which in turn raises a uncertainty aspect of the degree of reliability of offshore WECSs. The maintenance costs for offshore wind turbines have been found to be nearly 30–40% of the comprehensive life costs of WECSs [2,3], thus increasing the final production costs.

Reducing the maintenance cost is a key element in operating and generating power from WECSs [4,5]. The optimal cost of operation of a WECS is achieved in two ways: (i) by using efficient design techniques to prevent the unbalancing of loads and maintaining a rated power output throughout the operation, which can be achieved through appropriate modelling of the wind turbine system; (ii) by developing suitable fault diagnosis and fault–control strategies that prevent unnecessary maintenance and have shorter shutdown period due to failure. Technological advancements have proposed and implemented several effective designs for an aerodynamic model of wind turbines in recent years. However, the existence of faults is inevitable in the operation of wind energy systems. Like any other industrial system, wind turbines are prone to failures. Mechanical, actuator and sensor failures are the most commonly occurring failures in a WECS. Field survey data indicate that actuators of wind turbines are the most vulnerable components of a WECS [5–7] Any faulty event in the actuators of the wind turbine control system results in deviation of the system from its objectives and causes damage to the system components. A fault will deteriorate the performance of the complete system, resulting in the unscheduled shutdown of the system. To remain operative and competitive, there is a high demand for improving the reliability and availability of wind turbines with reduced unscheduled down time in the electricity market, thus limiting O&M and reducing the final cost of energy.

Fault Detection and Isolation (FDI) could be considered as a phase or a by–product of Fault Tolerant Control (FTC). In general, FDI relies on three methods, *i.e.* parity equations, parameter estimation approaches and observer/filter methods [8]. Moreover, when the fault is estimated from the FDI module, it can be exploited for its compensation. Therefore, taking into account this strategy, two FTC methods can be also considered [9,10]: active FTC (AFTC) and passive FTC (PFTC) approaches [11–13].

FDI methods are used also in connection with FTC schemes because they can improve fault diagnosis performance. As an example, [14] proposed the design of a FDI/FTC scheme based on a fuzzy inference mechanism oriented to model uncertainties and actuator faults. A fault identification algorithm is addressed in [15] and applied to wind turbine pitch actuators. Other strategies designed through Lyapunov and Nussbaum–type functions are proposed in [16,17] to improve the operation of wind turbines.

FDI schemes for wind turbine faults were addressed with different approaches such as sliding mode approaches [18–20], fuzzy Takagi–Sugeno models [21–23], neural networks [24–26], neuro–fuzzy [27], linear observers [28–30], and Kalman filter [31–34].

These methods rely on online estimation and fault information, and any inaccurate information during faults may result in degradation of system performance and can cause instability during post–fault operation. This issue is of great significance in systems such as wind turbines having several sources of noise and uncertainties. The availability of the wind turbines must be ensured through effective FDI strategies and, thus, it is required to develop robust and reliable prognostic and diagnosis strategies in a WECS to ensure its safe operation.

With reference to this paper, the topic of the fault diagnosis of a wind turbine system is analysed. In particular, the design of practical and reliable solutions to FDI are considered. However, differently from other works by the same authors, the FTC topic is not investigated here, even if it can rely on the same tools exploited in this paper. In fact,

Preprints (www.preprints.org) | NOT PEER-REVIEWED | Posted: 13 May 2021 doi:10.20944/preprints202105.0315.v1

as already remarked above, the fault diagnosis module provides the reconstruction of the fault signal affecting the process, which could be actively compensated by means of a controller accommodation mechanism. Moreover, the fault diagnosis design is enhanced by the derived fault reconstructors that are estimated via data–driven approaches, as they also allow to accomplish the fault isolation task.

The first data–driven strategy proposed in this work exploits Takagi–Sugeno (TS) fuzzy prototypes [35,36], which are estimated via a clustering algorithm and exploiting the data–driven algorithm developed in [37]. For comparison purpose, a further approach is designed, which exploits Neural Networks (NNs) to derive the nonlinear dynamic relations between the input and output measurements acquired for the process under diagnosis and the faults affecting the plant. The selected structures belong to the feed–forward Multi–Layer Perceptron (MLP) neural network class that include also Auto–Regressive with eXogenous (ARX) inputs in order to model nonlinear dynamic links among the data. In this way, the training of these Nonlinear ARX (NARX) prototypes for fault estimation can exploit standard back–propagation training algorithm, as recalled *e.g.* in [38].

The designed fault diagnosis schemes are tested via a high–fidelity simulator of a wind turbine process, which describes its behaviour in healthy and faulty conditions. This simulator, which represents a benchmark [39], includes the presence of uncertainty and disturbance effects, thus allowing to verify the reliability and robustness characteristics of the proposed fault diagnosis methodologies. Moreover, this work proposes to validate the efficacy of the designed fault diagnosis techniques by exploiting a more realistic scenario, which consists of a Hardware–In–the–Loop (HIL) tool.

It is worth noting the main contributions of this paper with respect to previous works by the authors. For example, this study analyses the solutions addressed *e.g.* in [40] but taking into account a more realistic and real–time system illustrated in Section 4. On the other hand, the fault diagnosis scheme developed in this paper was designed for a wind turbine system also in [41], but without considering the HIL environment.

The fuzzy methodology was also proposed by the authors in [42], which considered the development of recursive algorithms for the implementation of adaptive laws relying on Linear Parameter Varying (LPV) systems. The approach proposed in this paper estimates the fault diagnosis models by means of off–line procedures. Moreover, this paper further develops the achievements obtained *e.g.* in [43], but concerning the fault diagnosis a wind farm. The paper [44] proposed the design of a fault tolerant controller using the input–output data achieved from a single wind turbine, by exploiting the results achieved in [41,45]. On the other hand, this work considers the verification and the validation of the proposed fault diagnosis methodologies by exploiting an original HIL tool, proposed considered in a preliminary paper by the same authors [46,47].

The work follows the structure sketched in the following. Section 2 briefly summarises the wind turbine simulator, as it represents a well-established benchmark available in literature [48]. Section 3 describes the fault diagnosis strategies based on Fuzzy Systems (FSs) and Neural Network (NN) structures, detailed in Section 3.1. Section 4 summarises the obtained results via extended simulations, whilst Section 4.1 illustrates the HIL tool describing the behaviour of the wind turbine process. Finally, Section 5 concludes the work by reporting the main points of the paper and suggesting some interesting issues for further research and future investigations.

2. Wind Turbine Model Description

This section illustrates the Wind Turbine (WT) benchmark considered in this work. Moreover, Section 2.1 sketches the procedure exploited for the selection of the input and output measurements that feed the residual generators for FDI, as recalled in Section 3.

The WT simulator exploited in this work for validation purposes was earlier presented in [39,48] and motivated by an international competition. Despite its quite simple structure, it is able to describe quite accurately the actual behaviour of a three–blade

Preprints (www.preprints.org) | NOT PEER-REVIEWED | Posted: 13 May 2021 doi:10.20944/preprints202105.0315.v1

horizontal–axis wind turbine that is working at variable–speed and it is controlled by means of the pitch angle of its blades. The plant includes several interconnected subsystems, namely the wind process, the wind turbine aerodynamics, the drive–train, the electric generator/converter, the sensor and actuator systems and the baseline controller. The overall system is sketched in Figure 1, which represents the fault diagnosis target developed in this work. Further details of the WT benchmark will not be provided here, as they were described in detail in [4] and the references therein.

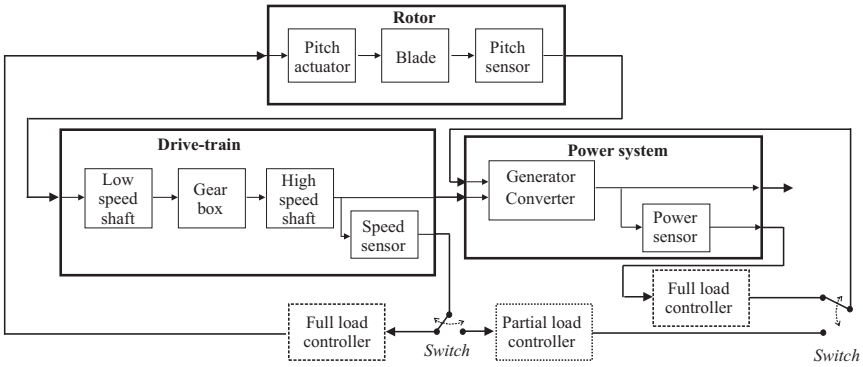

Figure 1. The WT benchmark and its functional subsystems.

This wind turbine benchmark is able to generate different typical fault cases affecting the sensors, the actuators and the process components. This scenario comprising 9 faulty situations is illustrated in Section 2.1, which describes the procedure for determining the input and output measurements acquired from the WT process and mainly affected by these faults.

2.1. Fault Sensitivity Analysis

The paper proposes to exploit this tool, which was suggested earlier by the authors for different applications, see *e.g.* [49,50] , as it simplifies the design of the bank of fault estimators as well as enhances the identification of the dynamic FS and NN prototypes recalled in Section 3.1. Moreover, this analysis must be preliminary performed on the WT simulator. In particular, as already remarked, it is used to select the input and output measurements $u_j(k)$ and $y_l(k)$ of the process that feed the dynamic FIS or NN of the bank of Figure 3.

In practice, the actuator faults considered in the WT benchmark have been injected into the simulator, assuming that only a single fault may occur. Then, the Relative Mean Square Errors (RMSE) index computed by considering the fault–free and faulty measured signals is computed, so that, for each fault, the most sensitive signal $u_j(k)$ and $y_l(k)$ is determined.

In particular, the fault sensitivity analysis relies on a selection algorithm using the normalised sensitivity function N_x in the form of Eq. 1:

$$N_x = \frac{S_x}{S_x^*} \tag{1}$$

with:

$$S_x = \frac{\left\| x_f(k) - x_n(k) \right\|_2}{\| x_n(k) \|_2} \tag{2}$$

and:

$$S_x^* = \max \frac{\left\| x_f(k) - x_n(k) \right\|_2}{\| x_n(k) \|_2} \tag{3}$$

The factor N_x represents the effect of the considered fault case on the generic measured signal $x(k)$, with $k = 1, 2, \ldots, N$ its sample number. The subscripts 'f' and 'n' indicate

Preprints (www.preprints.org) | NOT PEER-REVIEWED | Posted: 13 May 2021 doi:10.20944/preprints202105.0315.v1

the faulty and the fault–free case, respectively. Therefore, the signals mainly affected by the considered fault generate a value of N_x equal to 1. On the other hand, values of N_x closer to zero indicate that $x(k)$ is not affected by the fault. Those signals corresponding to significantly higher values of N_x are thus selected as the most sensitive measurements to the fault cases, and will used to feed the fault diagnosis modules of the bank reported in Figure 3.

As already remarked, the WT benchmark is able to generate different typical fault cases affecting the sensors, the actuators and the process components. This scenario comprising 9 fault situations is illustrated by means of Table 1, which reports the input and output measurements acquired form the WT process signals and mainly affected by these faults. In particular, Table 1 summarises the results of this fault sensitivity analysis for the case of the WT simulator.

Table 1: Fault scenario of the WT benchmark.

Fault Case	Fault Type	Most Affected Input–Output Measurements
1	Sensor	$\beta_{1,m1}$, $\beta_{1,m2}$, $\omega_{g,m2}$
2	Sensor	$\beta_{1,m2}$, $\beta_{2,m2}$, $\omega_{g,m2}$
3	Sensor	$\beta_{1,m2}$, $\beta_{3,m1}$, $\omega_{g,m2}$
4	Sensor	$\beta_{1,m2}$, $\omega_{g,m2}$, $\omega_{r,m1}$
5	Sensor	$\beta_{1,m2}$, $\omega_{g,m2}$, $\omega_{r,m2}$
6	Actuator	$\beta_{1,m2}$, $\beta_{2,m1}$, $\omega_{g,m2}$
7	Actuator	$\beta_{1,m2}$, $\beta_{3,m2}$, $\omega_{g,m2}$
8	Actuator	$\beta_{1,m2}$, $\tau_{g,m}$, $\omega_{g,m2}$
9	System	$\beta_{1,m2}$, $\omega_{g,m1}$, $\omega_{g,m2}$

In this way, Table 1 reports the most sensitive measurements $u_j(k)$ and $y_l(k)$ acquired from the WT system with respect to the fault conditions implemented in the WT benchmark. In practice, the fault signals of Table 1 were injected into the WT simulator, assuming that only a single fault may occur. Then, by checking the Relative Mean Square Errors (RMSEs) between all the fault–free and faulty measurements from the WT plant, the most sensitive signal $u_j(k)$ and $y_l(k)$ was selected and reported in Table 1.

For FDI purpose, the complete model of the WT benchmark can be described as a nonlinear continuous–time dynamic model represented by the function $\mathbf{f}_{wt}$ of Eq. (4) including the overall behaviour of the WT process reported in Figure 1 with state vector $\mathbf{x}_{wt}$ and fed by the driving input vector $\mathbf{u}$:

$$\begin{cases} \dot{\mathbf{x}}_{wt}(t) &= \mathbf{f}_{wt}(\mathbf{x}_{wt}, \mathbf{u}(t)) \\ \mathbf{y}(t) &= \mathbf{x}_{wt}(t) \end{cases} \tag{4}$$

Eq. (4) highlights that the simulator allows to measure all the state vector signals, *i.e.* the rotor speed, the generator speed and the generated power of the WT process:

$$\mathbf{x}_{wt}(t) = \mathbf{y}(t) = \left[\omega_{g,m1},\ \omega_{g,m2},\ \omega_{r,m1},\ \omega_{r,m2},\ P_{g,m}\right]$$

The driving input vector is represented by the following signals:

$$\mathbf{u}(t) = \left[\beta_{1,m1},\ \beta_{1,m2},\ \beta_{2,m1},\ \beta_{2,m2},\ \beta_{3,m1},\ \beta_{3,m2},\ \tau_{g,m}\right]$$

that represent the acquired measurements of the pitch angles from the three WT blades and the measured generator/converter torque. These signals are acquired with sample time T in order to obtain N data indicated as $\mathbf{u}(k)$ and $\mathbf{y}(k)$ with index $k = 1, \ldots, N$ that are exploited to design the FDI strategies addressed in this work.

Note finally that this tool represents one of the key features of the proposed strategy to FDI. In fact, the fault estimators exploited for FDI can be estimated by using a smaller

Preprints (www.preprints.org) | NOT PEER-REVIEWED | Posted: 13 May 2021 doi:10.20944/preprints202105.0315.v1

number of inputs, thus leading to a noteworthy simplification of the overall complexity, while decreasing the computational cost of the training algorithms.

3. Data–Driven Strategies for Fault Diagnosis

This section recalls the fault diagnosis strategy proposed in this paper that relies on FS and NN tools, as summarised in Section 3.1. These architectures are able to represent NARX models exploited for estimating the nonlinear dynamic relations between the input and output measurements of the WT process and the fault signals. In this sense, these NARX prototypes will be employed as fault estimators for solving the problem of the fault diagnosis of the WT system.

Under these assumptions, the fault estimators derived by means of a data–driven approach represent the residual generators $\mathbf{r}(k)$, which provide the on–line reconstruction $\hat{\mathbf{f}}(k)$ of the fault signals summarised in Table 1, as represented by Eq. (5):

$$\mathbf{r}(k) = \hat{\mathbf{f}}(k) \tag{5}$$

where the term $\hat{\mathbf{f}}(k)$ represents the general fault vector of Table 1, *i.e.* $\hat{\mathbf{f}}(k) = \{\hat{f}_1(k), \ldots \ldots, \hat{f}_9(k)\}$.

The fault diagnosis scheme exploiting the proposed fault estimators as residual generator is sketched in Fig. 2. Note that, as already highlighted, this scheme is also able to solve the fault isolation task [8].

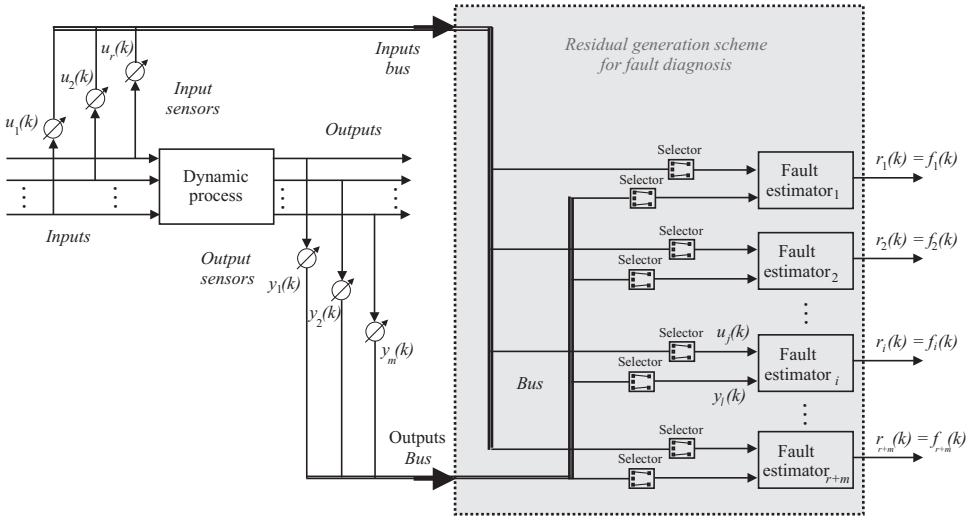

Figure 2. Bank of fault reconstructors for FDI.

Figure 2 shows that the general residual generator exploits the input and output measurements acquired from the process under diagnosis, $\mathbf{u}(k)$ and $\mathbf{y}(k)$, properly selected according to the analysis shown in Table 1. The fault detection problem can be easily achieved by means of a simple threshold logic applied to the residuals themselves, as described in [8]. This issue will not be considered in this paper.

Once the fault detection phase is solved, the fault isolation stage is directly obtained via the the bank of estimators of Figure 2. In this case, the number of estimators of Figure 2 is equal to the faults to be detected, *i.e.* 9, which is lower than the number of input and output measurements, $r + m$, acquired from the WT process.

This condition provides several degrees of freedom, as the i–th reconstructor of the fault $\hat{f}(k) = r_i(k)$ is a function of the input and output signals $\mathbf{u}(k)$ and $\mathbf{y}(k)$. These signals are thus selected in order to be affected sensitive to the specific fault $f_i(k)$, as highlighted in Table 1. This procedure enhances also the design of the fault reconstructors, as it reduces the number of possible input and output measurements, $u_j(k)$ and $y_l(k)$, which have to be considered for the identification procedure reported in Section 3.1.

Preprints (www.preprints.org) | NOT PEER-REVIEWED | Posted: 13 May 2021 doi:10.20944/preprints202105.0315.v1

The sensitivity analysis already represented in Table 1 has to be performed before the estimation of the fault estimators. Therefore, once the input–output signals are selected, according to Table 1, the FSs and the NNs used as fault reconstructors can be developed, as summarised in Section 3.1.

3.1. Fault Estimators via FS and NN Tools

This section recalls the procedure for developing the fault estimators modelled as Takagi–Sugeno (TS) FSs. In this way, the unknown dynamic relations between the selected input and output measurements of the WT plant and the faults are represented by means of FSs, which rely on a number of rules, antecedent and consequent functions. These rules are used to represent the inference system for connecting the measured signals from the system under diagnosis to its faults, in form of IF $\Longrightarrow$ THEN relations, implemented via the so–called Fuzzy Inference System (FIS) [35].

According to this modelling strategy, the general TS fuzzy prototype has the of Eq. (6):

$$\hat{f}(k) = \frac{\sum_{i=1}^{n_C} \lambda_i(\mathbf{x}(k)) \left(\mathbf{a}_i^T \mathbf{x}(k) + b_i\right)}{\sum_{i=1}^{n_C} \lambda_i(\mathbf{x}(k))} \tag{6}$$

Using this approach, in general, the fault signal $\hat{f}(k)$ is reconstructed by using suitable data taken from the WT process under diagnosis. In this case, the fault function $\hat{f}(k)$ is represented as a weighted average of affine parametric relations $\mathbf{a}_i^T \mathbf{x}(k) + b_i$ (consequents) depending on the input and output measurements collected in $\mathbf{x}(k)$. These weights are the fuzzy membership degrees $\lambda_i(\mathbf{x})$ of the system inputs.

The parametric relations of the consequents depend on the unknown variables $\mathbf{a}_i$ and b_i, which are estimated by means of an identification approach. The rule number is assumed equal to the cluster number n_C exploited to partition the data via a clustering algorithm with respect to regions where the parametric relations (consequents) hold [35].

Note that the system under diagnosis corresponds to a WT plant, which is described by a dynamic model. Therefore, the vector $\mathbf{x}(k)$ in Eq. (6) contains both the current and the delayed samples of the system input and output measurements. Therefore, the consequents includes discrete–time linear Auto–Regressive with eXogenous (ARX) input structures of order o. This regressor vector is described in form of Eq. (7):

$$\mathbf{x}(k) = \left[\ldots, y_l(k-1), \ldots, y_l(k-o), \ldots u_j(k), \ldots, u_j(k-o), \ldots\right]^T \tag{7}$$

where $u_l(\cdot)$ and $y_j(\cdot)$ represent the l–th and j–th components of the actual WT input and output vectors $\mathbf{u}(k)$ and $\mathbf{y}(k)$. These components are selected according to the results reported in Table 1.

The consequent affine parameters of the i–th model of the Eq. (6) are usually represented with a vector:

$$\mathbf{a}_i = \left[\alpha_1^{(i)}, \ldots, \alpha_o^{(i)}, \delta_1^{(i)}, \ldots, \delta_o^{(i)}\right]^T \tag{8}$$

where usually the coefficients $\alpha_j^{(i)}$ are associated to the delayed output samples, whilst $\delta_j^{(i)}$ to the input ones.

The approach proposed in this paper for the derivation of the generic i–th fault approximator (FIS) starts with the fuzzy clustering of the data $\mathbf{u}(k)$ and $\mathbf{y}(k)$ from the WT process. This paper exploits the well-established Gustafson–Kessel (GK) algorithm [35]. Moreover, the estimation of the FIS parameters is addressed as a system identification problem from the noisy data of the WT process. Once the data are clustered, the identification strategy proposed in this work exploits the methodology developed by the authors in [51].

Preprints (www.preprints.org) | NOT PEER-REVIEWED | Posted: 13 May 2021 doi:10.20944/preprints202105.0315.v1

Another key point not addressed in this work concerns the selection of the optimal cluster number n_C. This issue was investigated and developed by the authors, which leads to the estimation of the membership degrees $\lambda_i(\mathbf{x}(k))$ required in Eq. (6) and solved as a curve fitting problem [35].

This paper considers an alternative data–driven approach, which exploits neural networks used as fault approximators in the scheme of Figure 2. Therefore, in the same way of the fuzzy scheme, the bank of NNs is exploited to reconstruct the faults affecting the WT system under diagnosis using a proper selection of the input and the output measurements. The exploited NN structure consists of a feed–forward Multi–Layer Percepron (MLP) architecture with 3 layers of neurons [38].

However, as MPL networks represent static relations, the paper suggests to implement the MLP structure with a tapped delay line. Therefore, this quasi–static NN represents a powerful way for estimating nonlinear dynamic regressions between the input and output measurements from the WT process and its fault functions. This solution allows to obtain another Nonlinear ARX (NARX) description among the data. Moreover, when properly trained, these NARX NNs are able to reconstruct the fault function $\hat{f}(k)$ using a suitable selection of the past measurements of the WP system inputs and outputs $u_l(k)$ and $y_j(k)$, respectively. The example of the general solution is sketched in Figure 3, which can be implemented by means of FIS or NARX NN structures.

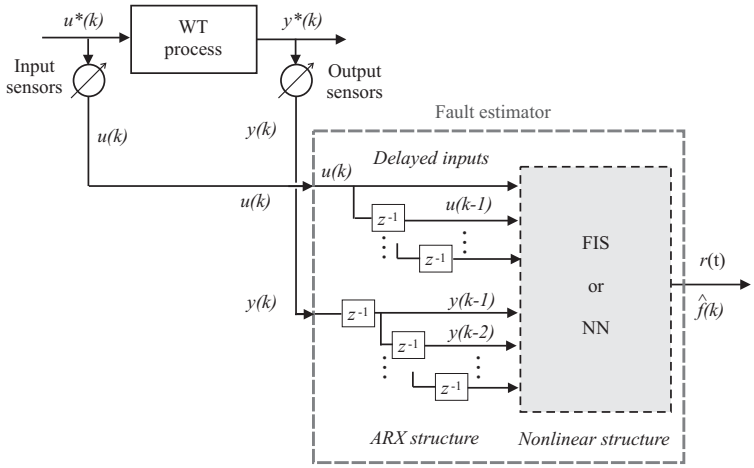

Figure 3. General scheme for fault reconstruction.

Similarly to the fuzzy scheme, with reference to the i–th fault reconstructor, a bank of NARX NNs is exploited, where the generic NARX system models the relation of Eq. (9):

$$\hat{f}(k) = F\big(\ldots, u_j(k), \ldots, u_j(k-d_u), \ldots y_l(k-1), \ldots, y_l(k-d_y), \ldots\big) \tag{9}$$

where $\hat{f}(k)$ represents the estimate of the general i–th fault in Table 1, whilst $u_j(\cdot)$ and $y_l(\cdot)$ indicate the components of the measured inputs and outputs of the WT process. These signals are selected again by means of the solution of the fault sensitivity problem reported in Table 1. The accuracy of the fault reconstruction depends on the number of neurons per layer, their weights and their activation functions. The results of the selection of the optimal structure of the fault reconstructors for FDI and the achieved performances will be shown in Section 4.

4. Simulation Results, Experimental Validation and Comparisons

With reference to the WT benchmark of Section 2, the simulations are driven by different wind sequences generated in a random way. They represent real measurements of wind speed sequences representing typical WT operating conditions, with ranges varying from 5 m/s. to 20 m/s. This scenario was modified by the authors with respect to the earlier benchmark proposed in [39]. The simulations consist of 4400 s., with single

Preprints (www.preprints.org) | NOT PEER-REVIEWED | Posted: 13 May 2021 doi:10.20944/preprints202105.0315.v1

fault occurrences and a number of samples $N = 440000$ for a sampling frequency of 100 Hz. Almost all fault signals are modelled as step functions lasting for 100 s. with different commencing times. Further details can be found in [39,48].

The first part of this section reports the results achieved by means of the fuzzy prototypes used as fault reconstructors according to Section 3.1. In particular, the fuzzy c–means and the GK clustering algorithms were exploited. A number of clusters $n_C = 4$ of clusters and a number of delays $o = 3$ were estimated. The membership functions of the TS FS and the parameters of the consequents $\alpha_j^{(i)}$ and $\delta_j^{(i)}$ were estimated for each cluster by following the procedure developed by the same authors in [52]. The TS FSs of Eq. (6) were thus determined and 9 fault reconstructors were organised according to the scheme of Figure 2.

The performances of the 9 TS FSs when used as fault estimators were evaluated again according to the RMSE % index, computed as the difference between the reconstructed $\hat{f}(k)$ and the actual $f(k)$ signals for each of the fuzzy estimators. These values were reported in Table 2.

Table 2: FS fault estimator capabilities.

Fault Case	1	2	3	4	5
RMSE%	1.61%	2.22%	1.95%	1.87%	1.92%
Sdt. Dev.	±0.02%	±0.03%	±0.01%	±0.01%	±0.01%
Fault Case	6	7	8	9	
RMSE%	2.15%	1.76%	2.13%	1.98%	
Sdt. Dev.	±0.02%	±0.01%	±0.02%	±0.01%	

Indeed, the RMSE % values reported in Table 2 represent an average of the results obtained from a campaign of 1000 simulations, as the benchmark exploited in this work changes the parameters of the WT model at each run. Moreover, the model–reality mismatch, the measurement errors, uncertainty and disturbance effects are described as Gaussian processes with suitable distributions, as remarked in Section 2. Therefore, Table 2 reports also the values of the standard deviation of the estimation errors achieved by the FS fault estimators.

Note that these reconstructed signals $\hat{f}(k)$ can be directly used as diagnostic residuals in order to detect and isolate the faults affecting the WT. Moreover, each TS FS of Eq. (6) is fed by 3 inputs (according to Table 1), with a number of delayed inputs and outputs $n = 3$ and $n_C = 4$ clusters.

As an example, Figure 4 shows the results regarding the fault cases 1, 2, 3, and 4 of the WT plant recalled in Section 2.

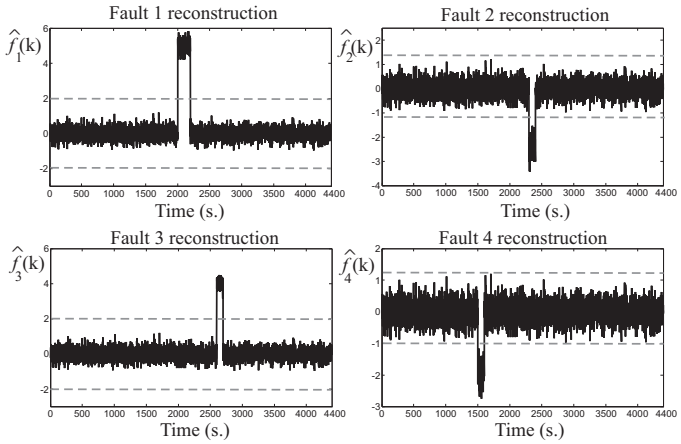

Figure 4. Reconstructed faults $\hat{f}(k)$ for cases 1, 2, 3, and 4.

Preprints (www.preprints.org) | NOT PEER-REVIEWED | Posted: 13 May 2021 doi:10.20944/preprints202105.0315.v1

In particular, Figure 4 reports the estimated faults $\hat{f}(k) = r_i(k)$ provided from the FSs in faulty conditions (black continuous line). They are compared with respect to the corresponding fault–free residuals (grey line). The fixed thresholds reported with dotted lines are used for fault detection. Note that the reconstructed fault functions $\hat{f}(k) = r_i(k)$ are different from zero also in fault–free conditions due to the measurement errors and the model-reality mismatch. This aspect serves to highlight the accuracy of the reconstructed signals provided by the estimated fuzzy models.

As for the FSs, 9 NARX NNs summarised in Section 3.1 were derived to provide the reconstruction of the 9 faults affecting the WT plant. In particular, the NARX were implemented as MLP NNs with 3 layers: the input layer consisted of 3 neurons, the hidden one used 10 neurons, whilst one neuron for the output layer. 4 delays were used in the relation of Eq. (9). Moreover, sigmoidal activation functions were used in both the input and the hidden layers, and a linear function for the output layer. With reference to Table 1, the NARX NNs were fed by 9 signals, representing the delayed inputs and outputs from the WT process.

As for the FSs, the prediction accuracy of the NARX NN was analysed by means of the RMSE % index and its average values summarised in Table 3.

Table 3: NN fault estimator capabilities.

Fault Case	1	2	3	4	5
RMSE %	0.91%	0.92%	0.94%	1.21%	1.17%
Sdt. Dev.	±0.01%	±0.01%	±0.01%	±0.02%	±0.01%
Fault Case	**6**	**7**	**8**	**9**	
RMSE %	1.61%	0.98%	0.95%	1.41%	
Sdt. Dev.	±0.01%	±0.01%	±0.01%	±0.02%	

As for the FS case, Table 3 reports also the values of the standard deviation of the estimation errors achieved by the NARX NN fault estimators.

Also in this case, Figure 5 depicts some of the residual signals $\hat{f}(k) = r_i(k)$ provided by the NARX NNs for the fault conditions 6, 7, 8, and 9, and compared with respect to the fixed detection thresholds (dotted lines).

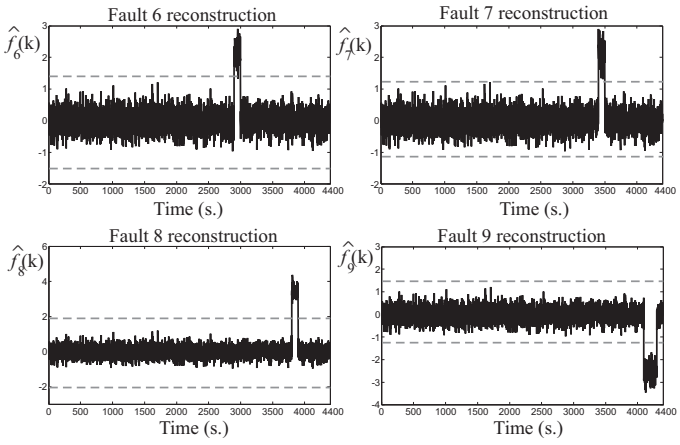

Figure 5. Estimated faults for cases 6, 7, 8, and 9.

Also in this case, the results obtained by the NARX NNs serve to highlight the efficacy of the developed solution, taking into account also disturbance and uncertainty affecting the WT system.

4.1. HIL Validation

In order to validate the developed fault diagnosis solutions in more realistic real–time working situations, the WT process and the designed algorithms have been im-

Preprints (www.preprints.org) | NOT PEER-REVIEWED | Posted: 13 May 2021 doi:10.20944/preprints202105.0315.v1

plemented and executed by means of a HIL tool. This test–bed allows to reproduce experimental tests that are oriented to the verification of the results achieved in simulations. This test–bed is sketched in Figure 6, which highlights its 3 main modules.

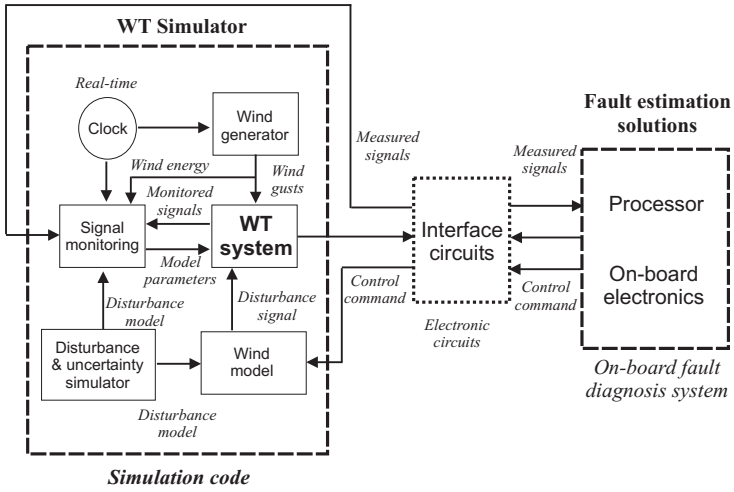

Figure 6. HIL tool for real–time validation.

The WT simulator that was used to describe WT system dynamics, its actuator, measurement sensors, and the WT controlled has been implemented in the LabVIEW environment. Realistic effects such as uncertainty, measurement errors, disturbance and the model–reality mismatch effects were also included, as recalled Section 2. The overall system is converted in the C++ code running on a standard PC, and allows also to test and monitor the signals generated by the proposed fault diagnosis strategies.

These fault diagnosis schemes summarised in Section 3.1 have been also compiled as executable code and implemented in an AWC 500 industrial system that features typical wind turbines requirements. This industrial module receives the signals acquired from the PC simulating the realistic WT plant that represent the monitored signals reported in Table 1. Therefore, the on board electronics elaborate these signals according to the fault diagnosis algorithms and produce the monitoring signals transmitted back to the WT simulator running on the PC.

An intermediate module represents the interface circuits providing the communications between the PC with the WT simulator and the on board electronics running the fault diagnosis algorithms. In this way, it manages the signals and exchanges the data between the WT simulator and the AWC 500 system.

The results achieved via this HIL tool are reported in Table 4 that summarises the capabilities of the fault diagnosis algorithms by means of the NSSE % performance index.

Table 4: RMSE % index for the HIL tool.

Fault Case	1	2	3	4	5
TS FSs	1.69%	2.29%	2.01%	1.94%	1.99%
NARX NNs	0.99%	0.98%	0.99%	1.28%	1.21%
Fault Case	6	7	8	9	
TS FSs	2.22%	1.81%	2.21%	2.03%	
NARX NNs	1.69%	1.02%	1.01%	1.51%	

Note that the tests summarised in Table 4 are consistent with the results reported in Tables 2 and 3. Although the accuracy of the simulations seems better than the performance achieved via the HIL tool, some remarks have to be drawn. First, the AWC 500 system uses calculations that are more restrictive than the PC simulator. Moreover, A/D and D/A devices are also exploited, which can introduce further deviations. On

Preprints (www.preprints.org) | NOT PEER-REVIEWED | Posted: 13 May 2021 doi:10.20944/preprints202105.0315.v1

the other hand, the testing of real scenarios does not involve the data transfer from a PC to on board electronics, thus reducing possible errors. Therefore, it can be finally remarked that the achieved results are quite accurate and motivate the application of the developed fault diagnosis strategies to real WT installations.

4.2. Comparative Analysis

To prove the features of the FDI performance of the proposed solutions, comparisons with other strategies are presented in this section. The developed FDI schemes are compared with methodologies already proposed by the same authors, relying on a model–based nonlinear approach, *i.e.* the so–called Adaptive Filter NonLinear Geometric Approach (NLGA–AF) [53] and a Recursive identification of Fuzzy Systems (RFS) [54]. Moreover, the Sliding Mode Observer (SMO) approach is also considered [20].

The performance of these three strategies is compared to the FDI methodologies (FS and NN) developed in this paper on the basis of the estimation accuracy through the experimental analysis, as shown in Table 5.

Table 5: RMSE % index for the HIL analysis and comparisons.

Fault Case	1	2	3	4	5	6	7	8	9
TS FSs	1.69%	2.29%	2.01%	1.94%	1.99%	2.22%	1.81%	2.21%	2.03%
NARX NN	0.99%	0.98%	0.99%	1.28%	1.21%	1.69%	1.02%	1.01%	1.51%
NLGA–AF	1.37%	1.45%	1.73%	1.75%	1.56%	1.99%	1.45%	1.54%	1.76%
RFS	1.99%	2.67%	2.44%	2.56%	2.67%	2.97%	2.23%	2.78%	2.82%
SMO	1.87%	1.82%	2.11%	2.01%	1.91%	2.34%	1.95%	2.08%	2.23%

According to the results summarised in Table 5, the performance of the ARX NN solution is higher than the ones obtained with the other schemes.

Moreover, it is worth noting that the values reported in Table 5 serve to assess the overall behaviour of the developed control techniques. In more detail, the values of the NSSE% index highlights that when the mathematical description of the dynamic process under investigation may be included in the design phase, the NLGA–AF technique with disturbance decoupling still yields to good performances, even if an optimisation procedure is required. However, when modelling errors are present, the offline learning feature of the data–driven fuzzy estimators TS FSs allows to achieve interesting results. For example, this consideration is valid also for the SMO estimators derived via a linearisation procedure. On the other hand, the fuzzy estimators TS FSs have led to more interesting capabilities. With reference to the adaptive scheme, such as the RFS, it takes advantage of its recursive features, since it is able to track possible variations of the system under diagnosis, due to operation or model changes. However, it requires quite complicated and not straightforward design procedures relying on data–driven recursive algorithms. Therefore, fuzzy–based schemes use the learning accumulated from data–driven offline simulations, but the training stage can be computationally heavy. Finally, concerning the NARX NN strategy, which represented the solution with the best results, it is rather simple and straightforward. Obviously, the achievable performances of linearised or adaptive methods are quite limited when applied to nonlinear dynamic processes. It can thus be concluded that the proposed data–driven approaches (NARX NN and TS FS) seem to represent powerful techniques able to cope with uncertainty, disturbance and variable working conditions.

5. Conclusion

This paper investigated fault diagnosis solutions that can be considered as viable and effective strategies for condition monitoring of a wind turbine process. To this end, the work proposed the design of fault estimators by means of data–driven methodologies relying on fuzzy models and neural networks. These solutions represented effective methods that allow the management of partially unknown information of the system dynamics, while coping with measurement errors, the model–reality mismatch

and other disturbance effects. Therefore, these data–driven methodologies were exploited to estimate nonlinear dynamic relations between the input and output process measurements and the faults. To this aim, the fuzzy and neural network prototypes integrated auto–regressive with exogenous input descriptions, thus making them able to approximate unknown nonlinear dynamic functions with arbitrary degree of accuracy. Once these models are derived for fault diagnosis purpose, their capabilities were verified and validated by using a high–fidelity benchmark that simulates the healthy and the faulty behaviour of a wind turbine system. The benchmark was also useful to analyse the robustness and the reliability characteristics of the developed tools in the presence of model–reality mismatch and measurement errors featured by the wind turbine simulator. Moreover, a hardware–in–the–loop tool was finally implemented for testing the performance of the developed fault diagnosis strategies in a more realistic environment. A comparative analysis with different fault diagnosis methods was also performed to demonstrate the better performance of the proposed dynamic neural strategy applied to the considered benchmark. The proposed design facilitated its derivation by using a data–driven training and learning algorithm that led to accurate fault identification and greater robustness. This solution saved the computing cost with reduced required iterations, easier design and implementation. The achieved results highlighted that data–driven approaches, such as fuzzy structures were able to provide good performances. However, they were easily outperformed by self–learning schemes, representing data–driven solutions that did not require optimisation stages, adaptation procedures or disturbance compensation methods. Further works will consider the application of the considered methodologies to real installations, in the presence of more realistic disturbance and uncertainty effects.

Author Contributions: Conceptualization, S.F. and S.S.; methodology, S.F.; software, S.F.; validation, S.F. and S.S.; formal analysis, S.S.; investigation, S.F.; resources, S.S.; data curation, S.F.; writing—original draft preparation, S.S.; writing—review and editing, S.S., S.F and P.C.; visualization, S.F.; supervision, S.S.; project administration, S.S. All authors have read and agreed to the published version of the manuscript.

Funding: This research received no external funding.

Conflicts of Interest: The authors declare no conflict of interest.

References

1. Liserre, M.; Cardenas, R.; Molinas, M.; Rodriguez, J. Overview of multi–mw wind turbines and wind parks. *IEEE Transactions on Industrial Electronics* **2011**, *58*, 1081–1095.
2. Byon, E.; Ntaimo, L.; Ding, Y. Optimal maintenance strategies for wind turbine systems under stochastic weather conditions. *IEEE Transactions on Reliability* **2010**, *59*, 393–404.
3. Besnard, F.; Bertling, L. An approach for condition–based maintenance optimization applied to wind turbine blades. *IEEE Transactions on Sustainable Energy* **2010**, *1*, 77–83.
4. Odgaard, P.F.; Stoustrup, J. A Benchmark Evaluation of Fault Tolerant Wind Turbine Control Concepts. *IEEE Transactions on Control Systems Technology* **2015**, *23*, 1221–1228.
5. Bianchi, F.D.; Battista, H.D.; Mantz, R.J. *Wind Turbine Control Systems: Principles, Modelling and Gain Scheduling Design*, 1st ed.; Advances in Industrial Control, Springer, 2007. ISBN: 1–84628–492–9.
6. Qiao, W.; Lu, D. A survey on wind turbine condition monitoring and fault diagnosis–part I: Components and subsystems. *IEEE Transactions on Industrial Electronics* **2015**, *62*, 6536–6545.
7. Hameed, Z.; Hong, Y.; Cho, Y.; Ahn, S.; Song, C. Condition monitoring and fault detection of wind turbines and related algorithms: A review. *Renewable and Sustainable Energy Reviews* **2009**, *13*, 1–39.
8. Chen, J.; Patton, R.J. *Robust Model–Based Fault Diagnosis for Dynamic Systems*; Kluwer Academic Publishers: Boston, MA, USA, 1999.
9. Mahmoud, M.; Jiang, J.; Zhang, Y. *Active Fault Tolerant Control Systems: Stochastic Analysis and Synthesis*; Lecture Notes in Control and Information Sciences, Springer–Verlag: Berlin, Germany, 2003. ISBN: 3540003185.
10. Zhang, Y.; Jiang, J. Bibliographical review on reconfigurable fault–tolerant control systems. *Annual Reviews in Control* **2008**, *32*, 229–252.
11. Carroll, J.; McDonald, A.; McMillan, D. Reliability comparison of wind turbines with DFIG and PMG drive trains. *IEEE Transactions on Energy Conversion* **2015**, *30*, 663–670.

12. Arani, M.F.M.; Mohamed, Y.A.I. Assessment and enhancement of a full–scale PMSG–based wind power generator performance under faults. *IEEE Transactions on Energy Conversion* **2016**, *31*, 728–739.
13. Sloth, C.; Esbensen, T.; Stoustrup, J. Active and Passive Fault–Tolerant LPV Control of Wind Turbines. Proceedings of the 2010 American Control Conference; , 2010; pp. 4640–4646.
14. Badihi, H.; Zhang, Y.; Hong, H. Wind turbine fault diagnosis and fault–tolerant torque load control against actuator faults. *IEEE Transactions on Control Systems Technology* **2015**, *23*, 1351–1372.
15. Wu, D.; Liu, W.; Song, J.; Shen, Y. Fault estimation and fault–tolerant control of wind turbines using the SDW–LSI algorithm. *IEEE Access* **2016**, *4*, 7223–7231.
16. Li, D.; Li, P.; Cai, W.; Song, Y.; Chen, H. Adaptive fault–tolerant control of wind turbines with guaranteed transient performance considering active power control of wind farms. *IEEE Transactions on Industrial Electronics* **2018**, *65*, 3275–3285.
17. Habibi, H.; Rahimi Nohooji, H.; Howard, I. Adaptive PID control of wind turbines for power regulation with unknown control direction and actuator faults. *IEEE Access* **2018**, *6*, 464–479.
18. Zhang, T.; Kong, X. Adaptive fault–tolerant sliding mode control for high–speed trains with actuator faults under strong winds. *IEEE Access* **2020**, *8*, 143902–143919.
19. Zhang, J.; Bennouna, O.; Swain, A.K.; Nguang, S.K. Detection and isolation of sensor faults of wind turbines using sliding mode observers. 2013 International Renewable and Sustainable Energy Conference – IRSEC, 2013, pp. 234–239.
20. Tan, C.P.; Edwards, C. Sliding mode observers for robust detection and reconstruction of actuator and sensor faults. *International Journal of Robust and Nonlinear Control* **2003**, *13*, 443–463.
21. Poschke, F.; Georg, S.; Schulte, H. Fault reconstruction using a Takagi–Sugeno sliding mode observer for the wind turbine benchmark. 2014 UKACC International Conference on Control (CONTROL), 2014, pp. 456–461.
22. Gerland, P.; Gross, D.; Schulte, H.; Kroll, A. Design of sliding mode observers for ts fuzzy systems with application to disturbance and actuator fault estimation. 49th IEEE Conference on Decision and Control (CDC), 2010, pp. 4373–4378.
23. Schulte, H.; Zajac, M.; Georg, S. Takagi–Sugeno sliding mode observer design for load estimation and sensor fault detection in wind turbines. 2012 IEEE International Conference on Fuzzy Systems, 2012, pp. 1–8.
24. Guo, P.; Fu, J.; Yang, X. Condition Monitoring and Fault Diagnosis of Wind Turbines Gearbox Bearing Temperature Based on Kolmogorov-Smirnov Test and Convolutional Neural Network Model. *Energies* **2018**, *11*. doi:10.3390/en11092248.
25. Yu, W.; Huang, S.; Xiao, W. Fault Diagnosis Based on an Approach Combining a Spectrogram and a Convolutional Neural Network with Application to a Wind Turbine System. *Energies* **2018**, *11*. doi:10.3390/en11102561.
26. Dybkowski, M.; Klimkowski, K. Artificial Neural Network Application for Current Sensors Fault Detection in the Vector Controlled Induction Motor Drive. *Sensors* **2019**, *19*. doi:10.3390/s19030571.
27. Zhou, Q.; Xiong, T.; Wang, M.; Xiang, C.; Xu, Q. Diagnosis and Early Warning of Wind Turbine Faults Based on Cluster Analysis Theory and Modified ANFIS. *Energies* **2017**, *10*. doi:10.3390/en10070898.
28. Kuhne, P.; Poschke, F.; Schulte, H. Fault estimation and fault–tolerant control of the fast NREL 5-MW reference wind turbine using a proportional multi–integral observer. *International Journal of Adaptive Control and Signal Processing* **2018**, *32*, 568–585.
29. Habibi, H.; Nohooji, H.R.; Howard, I. A neuro–adaptive maximum power tracking control of variable speed wind turbines with actuator faults. 2017 Australian and New Zealand Control Conference (ANZCC), 2017, pp. 63–68.
30. Kamal, E.; Aitouche, A.; Abbes, D. Robust fuzzy scheduler fault tolerant control of wind energy systems subject to sensor and actuator faults. *International Journal of Electrical Power Energy Systems* **2014**, *55*, 402–419.
31. Idrissi, I.; Chafouk, H.; El Bachtiri, R. Actuator fault diagnosis approach for doubly fed induction generator of wind turbine. 2019 4th Conference on Control and Fault Tolerant Systems (SysTol). IEEE, 2019, pp. 378–383.
32. Gholami, M.; Schioler, H.; Bak, T. Active fault diagnosis for hybrid systems based on sensitivity analysis and EKF. Proceedings of the 2011 American Control Conference, 2011, pp. 244–249.
33. Zhang, X.; Zhang, Q.; Zhao, S.; Ferrari, R.; Polycarpou, M.M.; Parisini, T. Fault detection and isolation of the wind turbine benchmark: an estimation–based approach. IFAC Proceedings Volumes of the 18th IFAC World Congress. IFAC, Elsevier, 2011, Vol. 44, pp. 8295–8300.
34. Kim, D.; Lee, D. Fault Parameter Estimation Using Adaptive Fuzzy Fading Kalman Filter. *Applied Sciences* **2019**, *9*. doi:10.3390/app9163329.
35. Babuška, R. *Fuzzy Modeling for Control*; Kluwer Academic Publishers: Boston, USA, 1998.
36. Harrabi, N.; Kharrat, M.; Aitouche, A.; Souissi, M. Control Strategies for the Grid Side Converter in a Wind Generation System Based on a Fuzzy Approach. *International Journal of Applied Mathematics and Computer Science* **2018**, *28*, 323–333.
37. Simani, S.; Fantuzzi, C.; Rovatti, R.; Beghelli, S. Parameter Identification for Piecewise Linear Fuzzy Models in Noisy Environment. *International Journal of Approximate Reasoning* **1999**, *1*, 149–167. Publisher: Elsevier.
38. Korbicz, J.; Koscielny, J.M.; Kowalczuk, Z.; Cholewa, W., Eds. *Fault Diagnosis: Models, Artificial Intelligence, Applications*, 1st ed.; Springer–Verlag: London, UK, 2004. ISBN: 3540407677.
39. Odgaard, P.F.; Stoustrup, J.; Kinnaert, M. Fault–Tolerant Control of Wind Turbines: A Benchmark Model. *IEEE Transactions on Control Systems Technology* **2013**, *21*, 1168–1182. ISSN: 1063–6536. DOI: 10.1109/TCST.2013.2259235.
40. Simani, S.; Farsoni, S.; Castaldi, P. Data–Driven Techniques for the Fault Diagnosis of a Wind Turbine Benchmark. *International Journal of Applied Mathematics and Computer Science – AMCS* **2018**, *28*, 247–268. DOI: 10.2478/amcs-2018-0018.

41. Simani, S.; Farsoni, S.; Castaldi, P. Fault Tolerant Control of an Offshore Wind Turbine Model via Identified Fuzzy Prototypes. Proceedings of the 2014 UKACC International Conference on Control (CONTROL); Whidborne, J.F., Ed.; UKACC (United Kingdom Automatic Control Council), IEEE: Loughborough University, Loughborough, UK, 2014; pp. 494–499. ISBN: 9781467306874. Special session invited paper. DOI: 10.1109/CONTROL.2014.6915188.
42. Simani, S.; Castaldi, P. Data–Driven Design of Fuzzy Logic Fault Tolerant Control for a Wind Turbine Benchmark. 8th IFAC Symposium on Fault Detection, Supervision and Safety of Technical Processes – SAFEPROCESS 2012; Astorga-Zaragoza, C.M.; Molina, A., Eds.; Instituto de Ingeniería, Circuito escolar, Ciudad Universitaria, CP 04510, México D.F., IFAC: Mexico City, Mexico, 2012; Vol. 8, pp. 108–113. Invited session paper. ISBN: 978–3–902823–09–0. ISSN: 1474–6670. DOI: 10.3182/20120829-3-MX-2028.00036.
43. Simani, S.; Farsoni, S.; Castaldi, P. Residual Generator Fuzzy Identification for Wind Farm Fault Diagnosis. Proceedings of the 19th World Congress of the International Federation of Automatic Control – IFAC'14; IFAC & South Africa Council for Automation and Control, IFAC: Cape Town, South Africa, 2014; Vol. 19, pp. 4310–4315. Invited paper for the special session "FDI and FTC of Wind Turbines in Wind Farms" organised by P. F. Odgaard and S. Simani. DOI: 10.3182/20140824–6–ZA–1003.00052.
44. Simani, S.; Farsoni, S.; Castaldi, P. Active Fault Tolerant Control of Wind Turbines Using Identified Nonlinear Filters. Proceedings of the 2nd International Conference on Control and Fault–Tolerant Systems – SysTol'13; Control Systems Society, I., Ed.; Centre de Recherche en Automatique de Nancy – CRAN, IEEE: Nice, France, 2013; pp. 383–388. Special session invited paper. ISBN: 978–1–4799–2854–5. DOI: 10.1109/SysTol.2013.6693827.
45. Simani, S.; Farsoni, S.; Castaldi, P. Residual Generator Fuzzy Identification for Wind Turbine Benchmark Fault Diagnosis. *Machines* **2014**, *2*, 275–298. ISSN: 2075–1702. Special issue invited paper "Machinery Diagnostics and Prognostics". DOI: 10.3390/machines2040275.
46. Simani, S. Application of a Data–Driven Fuzzy Control Design to a Wind Turbine Benchmark Model. *Advances in Fuzzy Systems* **2012**, *2012*, 1–12. Invited paper for the special issue: Fuzzy Logic Applications in Control Theory and Systems Biology (FLACE) . ISSN: 1687–7101, e–ISSN: 1687-711X. DOI: 10.1155/2012/504368.
47. Simani, S.; Castaldi, P. Intelligent Fault Diagnosis Techniques Applied to an Offshore Wind Turbine System. *Applied Sciences* **2019**, *9*, 1–16. DOI: 10.3390/app9040783.
48. Odgaard, P.F.; Stoustrup, J.; Kinnaert, M. Fault Tolerant Control of Wind Turbines – a Benchmark Model. Proceedings of the 7th IFAC Symposium on Fault Detection, Supervision and Safety of Technical Processes; , 2009; Vol. 1, pp. 155–160. DOI: 10.3182/20090630–4–ES–2003.0090.
49. Simani, S.; Patton, R.J. Fault diagnosis of an industrial gas turbine prototype using a system identification approach. *Control Engineering Practice* **2008**, *16*, 769–786. Publisher: Elsevier Science. ISSN: 0967–0661. DOI: 10.1016/j.conengprac.2007.08.009.
50. Simani, S.; Farsoni, S. *Fault Diagnosis and Sustainable Control of Wind Turbines: Robust data–driven and model–based strategies*, 1st ed.; Mechanical Engineering, Butterworth–Heinemann – Elsevier: Oxford (UK), 2018. ISBN: 9780128129845.
51. Fantuzzi, C.; Simani, S.; Beghelli, S.; Rovatti, R. Identification of piecewise affine models in noisy environment. *International Journal of Control* **2002**, *75*, 1472–1485. Publisher: Taylor and Francis, Ltd. DOI: 10.1109/87.865858.
52. Rovatti, R.; Fantuzzi, C.; Simani, S. High–speed DSP–based implementation of piecewise–affine and piecewise–quadratic fuzzy systems. *Signal Processing Journal. Publisher: Elsevier* **2000**, *80*, 951–963. Special Issue on Fuzzy Logic applied to Signal Processing. DOI: 10.1016/S0165-1684(00)00013–X.
53. Simani, S.; Castaldi, P. Active Actuator Fault Tolerant Control of a Wind Turbine Benchmark Model. *International Journal of Robust and Nonlinear Control* **2014**, *24*, 1283–1303. John Wiley. DOI: 10.1002/rnc.2993.
54. Simani, S.; Castaldi, P. Data–Driven and Adaptive Control Applications to a Wind Turbine Benchmark Model. *Control Engineering Practice* **2013**, *21*, 1678–1693. Special Issue Invited Paper. ISSN: 0967–0661. PII: S0967–0661(13)00155–X. DOI: http://dx.doi.org/10.1016/j.conengprac.2013.08.009.